Inorganic Materials, Vol. 37, No. 9, 2001, pp. 871–885. Translated from Neorganicheskie Materialy, Vol. 37, No. 9, 2001, pp. 1031–1046.

Van der Waals Radii of Elements

S. S. Batsanov

Center for High Dynamic Pressures, Mendeleevo, Solnechnogorskii raion, Moscow oblast, 141570 Russia

Received February 14, 2001

Abstract—The available data on the van der Waals radii of atoms in molecules and crystals are summarized. The nature of the continuous variation in interatomic distances from van der Waals to covalent values and the mechanisms of transformations between these types of chemical bonding are discussed.

INTRODUCTION

The notion that an interatomic distance can be thought of as the sum of atomic radii was among the most important generalizations in structural chemistry, treating crystals and molecules as systems of interacting atoms (Bragg, 1920). The next step forward in this area was taken by Mack [1] and Magat [2], who introduced the concept of nonvalent radius (R) for an atom situated at the periphery of a molecule and called it *the atomic domain radius* [1] or *Wirkungsradius* [2], implying that this radius determines intermolecular distances. Later, Pauling [3] proposed to call it *the van der Waals radius*, because it characterizes van der Waals interactions between atoms. He also showed that the van der Waals radii of nonmetals coincide with their ionic radii and exceed their covalent radii (r), typically by 0.8 Å.

Initially, only x-ray diffraction (XRD) data, molar volume measurements, and crystal-chemical considerations were used to determine R. Later studies extended the range of experimental approaches and culminated in a complete system of the van der Waals radii of free and bound atoms. Comparison of the results obtained by various physical methods made it possible to assess the accuracy and locate the applicability limits of the van der Waals radii and to reconcile the concept of van der Waals radius with the quantum-mechanical requirement that the electron density vary continuously at the periphery of atoms.

In this review, the van der Waals radii of atoms evaluated from XRD data, molar volumes, physical properties, and crystal-chemical considerations are used to develop a universal system of van der Waals radii.

ISOTROPIC CRYSTALLOGRAPHIC VAN DER WAALS RADII

Kitaigorodskii [4, 5] was the first to formulate the principle of close packing of molecules in crystalline phases. He assumed that the van der Waals areas of peripheral atoms in neighboring molecules are in contact but do not overlap (rigid-atom model), because the repulsive forces between closed electron shells rise sharply with decreasing intermolecular distance. He made up a system of van der Waals radii as consistent as possible with the intermolecular distances in organic compounds. His radii differed little from Pauling's (Table 1).

The system of van der Waals radii was further refined by Bondi [6, 7]. His detailed tables were very popular among chemists, even though the values of R were criticized in a number of works [8]. Bondi not

Table 1. Crystallographic van der Waals radii of nonmetals

Author, year	R, Å								
	H	F	Cl	Br	I	O	S	N	C
Pauling, 1939	1.2	1.35	1.80	1.95	2.15	1.40	1.85	1.5	1.70
Bondi, 1964	1.20	1.47	1.75	1.85	1.98	1.52	1.80	1.55	1.70
Zefirov, 1974	1.16	1.40	1.90	1.97	2.14	1.29	1.84	1.50	1.71
Gavezzotti, 1983–1999	1.17	1.35	1.80	1.95	2.10	1.40	1.85	1.50	1.70
Batsanov, 1995			1.80	1.90	2.10	1.51	1.80		1.68
Wieberg, 1995		1.5	1.8	1.9	2.1	1.5	1.8	1.6	1.7
Rowland, 1996	1.10	1.46	1.76	1.87	2.03	1.58	1.81	1.64	1.77

0020-1685/01/3709-0871$25.00

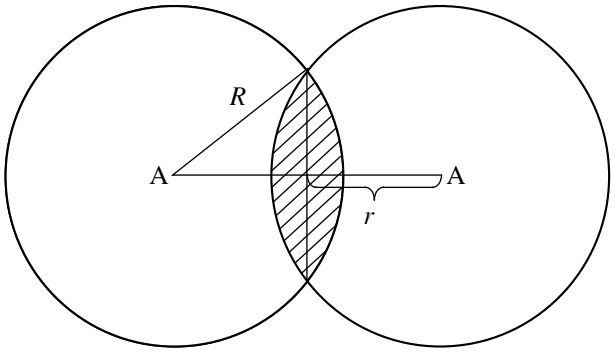

Fig. 1. Schematic showing the formation of an A_2 molecule.

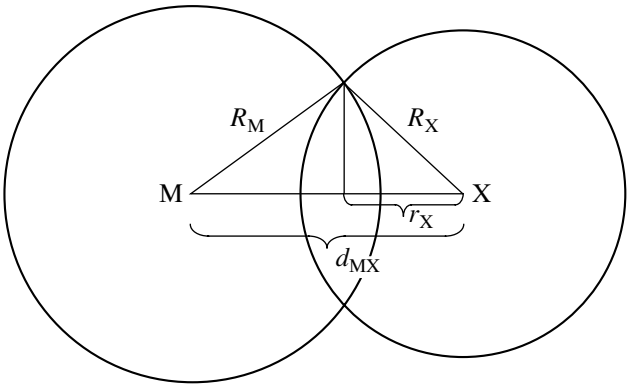

Fig. 2. Schematic showing the formation of an M–X bond.

only determined *R* from structural data but also calculated *R* by adding 0.76 Å to covalent radii and evaluated *R* from thermodynamic and physical properties. The *R* values recommended by Bondi are also listed in Table 1.

Zefirov and Zorkii [9, 10] corrected some of the van der Waals radii and made a number of new suggestions, in particular, that *R* should be calculated from the shortest intermolecular distances (*D*), ensuring a three-dimensional system of contacts, since other peripheral atoms of the molecule may be not in contact, and the determination of *R* by averaging all intermolecular distances may be unjustified. Although they highlight the statistical nature of van der Waals radii and their variability within a few tenths of an ångström, depending on various structural factors, the radii in their system are given with an accuracy of a few thousandths of an ångström (Table 1).

A classical approach to the determination of the van der Waals radii of organogens was proposed in [11–14] (Table 1). The system of van der Waals radii of nonmetals elaborated by Rowland and Taylor [15] for structural organic chemistry was based on a wealth of statistical data.

The van der Waals radii of the halogens and carbon in inorganic compounds were first determined by Pauling [3], who used data on layered compounds such as $CdCl_2$ and graphite. Later, the van der Waals radii of halogens and chalcogens were evaluated from a large body of experimental data [16]: OH 1.51, Cl 1.80, Br 1.90, I 2.10, S 1.80, Se 1.85, and Te 2.02 Å.

The van der Waals radii of metals are difficult to determine directly, because there is only a small number of structures in which metal atoms can be in contact with another molecule; with the development of structural chemistry, the number of such structures increases. Table 2 lists the crystallographic van der Waals radii determined to date [16–19].

Recently, the van der Waals radii of metals were calculated from structural data for metals [17] and their molecular compounds [20, 21]. Let us outline these approaches and the obtained results.

Since the valence state of a metal remains unchanged upon a polymorphic transformation, while the bond number increases, the electron density redistributes between ligands,

$$\Delta V_1 = 2\Delta V_2 = 3\Delta V_3\ldots, \quad (1)$$

where ΔV is the volume common to the two atomic spheres (Fig. 1), and the subscripts specify the bond number. It is easily seen that

$$\Delta V = \frac{2}{3}\pi(R-r)^2(2R+r). \quad (2)$$

Given that, in polymorphic transformations, a decrease in the intermolecular contact area is accompanied by an increase in covalent bond length [22], to each coordination number N_c there correspond particular *R* and *r*. Therefore, Eq. (1) takes the form

$$(R_1-r_1)^2(2R_1+r_1) = 2(R_2-r_2)^2(R_2+r_2) = \ldots, \quad (3)$$

valid for univalent atoms. In the case of multivalent metals, the left-hand side of Eq. (3) should be multiplied by valence v if single-bond radii are used as *r* [3]. As a result, we obtain

$$(R_1-r_1)^2(R_1+r_1) = n(R_n-r_n)^2(R_n+r_n), \quad (4)$$

where $n = N_c/v$. Taking into account that the maximal N_c in metals is 12, one can use Eq. (4) to calculate *R* corresponding to the largest change in N_c upon the polymorphic transformation. Such calculations were carried out [17] under the assumption that, upon an increase in N_c, the decrease in *R* is proportional to the increase in *r* (Table 2).

In another approach to determining *R*, the M–X bond is also thought of as the region common to the atomic spheres M and X, with an internuclear distance d_{MX} (Fig. 2). It is easily seen that

$$R_M = (R_X^2 + d_{MX}^2 - 2d_{MX}r_M)^{1/2}. \quad (5)$$

Table 2. Crystallographic van der Waals radii of metals

Atom	*R*, Å							
	[17]	[20]	[21]		empirical		[25]	(9)
Li	2.24	2.25	2.24	2.05			2.1	
Na	2.57	2.40		2.39			2.3	
K	3.00	2.67		2.67			2.7	
Rb	3.12	2.78		2.76			2.8	
Cs	3.31	2.90		2.93	2.9	3.1	2.9	
Cu	2.00	2.16	2.14	2.09	1.9		1.9	
Ag	2.13	2.25	2.29		1.9		2.0	
Au	2.13	2.18					2.0	
Be	1.86	2.03	1.99	1.86			1.8	
Mg	2.27	2.22	2.25	2.10			2.2	
Ca	2.61	2.43		2.27	2.17		2.6	
Sr	2.78	2.54		2.40	2.36		2.7	
Ba	2.85	2.67		2.55	2.52		2.8	
Zn	2.02	2.09	2.16	2.12	2.1		2.0	
Cd	2.17	2.18	2.29				2.1	
Hg	2.17	2.15	2.28		1.75 [18]	1.95	2.1	
Sc	2.28	2.37		2.18			2.3	2.25–2.41
Y	2.45	2.47		2.38	1.8		2.4	2.33–2.46
La	2.51	2.58		2.59			2.6	2.30–2.44
B	1.74	1.87		1.72	1.7	1.83	1.75	1.91–2.00
Al	2.11	2.19	2.17	1.97	2.02		2.0	2.29–2.38
Ga	2.08	2.17	2.16	2.14	2.05		2.0	1.95–2.02
In	2.24	2.28	2.29	2.32			2.2	2.09–2.15
Tl	2.25	2.29		2.42	2.05	1.92	2.3	2.01–2.07
Ti	2.14	2.30		2.22	2.0		2.1	2.11–2.19
Zr	2.25	2.38		2.31	2.3		2.2	2.20–2.29
Hf	2.24	2.34		2.29			2.3	2.04–2.12
Si	2.06	2.06		2.19	2.15		1.95	2.10–2.22
Ge	2.13	2.10		2.22	2.0		2.0	1.91–2.02
Sn	2.29	2.21	2.29	2.40	2.2		2.2	2.02–2.10
Pb	2.36	2.24		2.46	2.3		2.3	2.00–2.08
V	2.03			2.14	2.0		2.0	2.05–2.19
Nb	2.13	2.34		2.15			2.1	1.96–2.10
Ta	2.13	2.26		2.22			2.2	1.93–2.05
As	2.16	2.05		2.14	1.96		2.0	1.92
Sb	2.33	2.20		2.32			2.2	2.06–2.10
Bi	2.42	2.28		2.40	2.22	2.40 [19]	2.4	2.04–2.08
Cr	1.97	2.27		2.05	2.0		2.0	2.06–2.20
Mo	2.06	2.29		2.16	2.2		2.1	1.92–2.00
W	2.07	2.23		2.14	2.2		2.1	1.85–1.93
Mn	1.96	2.15	2.23 [24]	2.00			2.0	2.00–2.14
Tc	2.04			2.11			2.1	1.93–2.02
Re	2.05	2.21		2.11			2.1	1.78–1.86
Fe	1.96	2.19		1.98	2.1		2.0	2.05–2.25
Co	1.95	2.16		1.97			2.0	1.94–2.14
Ni	1.94	2.14		1.97			2.0	1.88–2.11
Ru	2.02			2.05	2.16		2.1	1.89–1.97
Rh	2.02			2.04			2.1	1.83–1.90
Pd	2.05			2.14			2.1	1.87–1.96
Os	2.03			2.02			2.1	1.76–1.82
Ir	2.03			2.01			2.1	1.76–1.82
Pt	2.06			2.15	2.1	2.02	2.1	1.77–1.85
Th	2.43	2.54		2.50				2.25
U	2.17	2.51		2.45				1.94

* Minimal radius from M⋯H van der Waals distances for R(H) = 1.2 Å [32].

Using an orbital radius for r_X and knowing R_X, one can calculate R_M.

Since the metals in organic compounds are coordinated most frequently by C, S, N, Cl, and Br, with electronegativities $\chi_C = \chi_S$ and $\chi_N = \chi_{Cl}$, the R_M listed in Table 2 are averaged over the structures of $M(CH_3)_n$, MCl_n, and MBr_n [20]. Table 2 also gives the R_{Au} calculated from the recent data on the bond lengths in the AuCl and AuBr molecules [23].

The intermolecular contact radii R_{IC} were calculated in [21]. It was shown that the values of R_{IC} in tetrahedral crystals coincide with the van der Waals radii of the elements of the fifth period and their compounds (Table 2, left column under Ref. [21]). The contact radii determined from the $M\cdot\cdot C(CH_3)$ distances in $M(C_5Me_5)_n$ molecules coincide with or are close to the van der Waals radii determined by independent methods (Table 2, right column under Ref. [21]). The likely reason is that the CH_3 group deviates from the plane of the C_5 ring without significant energy changes, and, hence, the repulsion between M and $C(CH_3)$ is similar to the intermolecular interaction.

If the bond length d(M–X) is close to $r_M + r_X$ and $r_M \simeq r_X$, we obtain from Eq. (5) for tetrahedral structures

$$R = [d^2 + (0.8166d)^2 - 2dr]^{1/2} = 1.633r. \quad (6)$$

For $r \simeq 1.2$ Å (average radius of organogens), we obtain $R - r = 0.633 \times 1.2 = 0.76$ Å (the rule proposed by Pauling and confirmed by Bondi). The values of R calculated in [25] as $r + 0.8$ Å are also given in Table 2.

It can be seen in Fig. 1 that the overlap region, situated between symmetrically arranged, positively charged atomic cores, will extend perpendicular to the bond direction with decreasing bond length. This is supported by experimental data [26, 27]. From electrostatic considerations, it follows that the thickness of the high-electron-density region must increase with the distance from the bond line. Clearly, this effect will be more pronounced in the N_2, O_2, and F_2 molecules [28].

To which extent can the electron cloud be deformed? Clearly, electrons can be promoted no farther than to the next shell. Since the atomic size depends on the principal quantum number n,

$$r = a_0 n^2/Z^*, \quad (7)$$

where a_0 is the Bohr radius for hydrogen, and Z^* is the effective charge on the nucleus [3], the largest value of the atomic radius is

$$R = a_0(n+1)^2/Z^*. \quad (8)$$

Hence,

$$R/r = [(n+1)/n]^2. \quad (9)$$

Equation (9) can be used to calculate R from the known covalent radii of atoms in p_σ bonds. Table 2 summarizes the van der Waals radii calculated by Eq. (9) from the normal (minimal) and crystalline (maximal) covalent radii [29].

The scatter in the R of metals in Table 2 is due not only to experimental errors and inaccuracy in calculations but also to the effect of bond polarity, a positive charge which reduces the size of the atom. It was found empirically [20, 21] that the van der Waals radius of a metal can be written as

$$R_{M(X)} = R^0_M - b\Delta\chi^m_{MX}, \quad (10)$$

where R^0_M is the van der Waals radius of an uncharged atom, $\Delta\chi_{MX}$ is the difference in electronegativity, and b and m are constants.

Whereas the radii of metals depend mainly on bond polarity, those of nonmetals are determined for the most part by the structural features of molecules, because they are close to the anion radii. Besides, since there is a relationship between R and r, and r depends on the valence of the atom, R also must depend on the valence, as shown by Pyykkö [18].

The variations in R across homologous series of molecules were examined using AX_4 tetrahalides as examples. The details of the calculations based on the principle of close packing are described in [30]; the

Table 3. Intermolecular contact (R_{IC}) and van der Waals (R) radii (Å) of halogens in AX_4 crystals

AX_4	$R_{IC}(X)$	$R(X)$	AX_4	$R_{IC}(X)$	$R(X)$
			CBr_4(I)	1.562	2.046
CF_4	1.073	1.548	CBr_4(II)	1.562	2.007
SiF_4	1.257	1.504	$GeBr_4$	1.855	2.062
GeF_4	1.379	1.398	$SnBr_4$	1.964	2.005
			CI_4	1.760	2.096
CCl_4(I)	1.448	1.957	SiI_4	1.984	2.209
CCl_4(II)	1.448	1.900	GeI_4	2.040	2.198
$SiCl_4$	1.640	1.906	SnI_4	2.178	2.176

Note: I and II are the cubic and monoclinic forms, respectively.

results are summarized in Table 3. The average van der Waals radii of halogens in tetrahalides agree with the values given in Table 1.

The data in Table 3 indicates the tendency for R_X to decrease in going from CX_4 to SnX_4 because of the stronger van der Waals interaction between molecules at larger electronic polarizabilities. A similar situation is observed in liquid tetrahalides:

MCl_4	CCl_4	$SiCl_4$	$GeCl_4$
R_{Cl}, Å [31]	1.75	1.63	1.53

Accordingly, the distance between the central atom of a molecule and the nearest atom X of the neighboring molecule also decreases in going from $SiCl_4$ to $GeCl_4$ and to $SnCl_4$: 4.90, 4.60, and 4.57 Å, respectively [32].

The van der Waals radii of halogens deduced from the structure of X_2 molecules in the liquid state are notably larger, since the polarizabilities of X_2 are higher than those of the corresponding AX_4 molecules:

X	F	Cl	Br	I
R_X, Å [33]	1.54	1.89	2.03	2.23

DETERMINATION OF VAN DER WAALS RADII FROM MOLAR VOLUMES OF SOLIDS

Since the van der Waals equation incorporates the molecular volume, imposing a lower limit to the intermolecular distance, this volume can be used to calculate the latter. Indeed, the molar volumes calculated from gas-kinetics data, molecular refractions, and van der Waals radii are in reasonable agreement [34] and can, therefore, be used in dealing with structural problems [4, 5, 35]. The determination of isotropic van der Waals radii from molar volumes in structures where the intermolecular distances are direction-dependent is the most appropriate procedure for averaging experimental data.

Treating atoms as rigid spheres, one can calculate the packing factor of molecules in crystals, which ranges, according to Kitaigorodskii [4, 5], from 0.65 to 0.77. As shown later, the packing factor in organic compounds can be much larger, up to $\rho = 0.9$ [10]. In complex molecules whose rigid structure prevents close packing, ρ is below that of close packing (0.74); the ρ values above 0.74 suggest that the concept of close packing should be revised. Indeed, the packing factor of homodesmic (diamond, β-Sn, bcc, or fcc) structures can be calculated as the ratio of the covalent atomic volume to the unit-cell volume per atom. The packing factor of heterodesmic (molecular) structures is equal to the ratio of the van der Waals molecular volume (sum of the van der Waals volumes of the constituent atoms) to the unit-cell volume per molecule. In view of this, strictly speaking, the packing factors of organic and inorganic structures cannot be compared.

However, one can combine the "organic" and "inorganic" concepts by taking into account the covalent and van der Waals contribution to ρ. As a first approximation, it can be taken that, in the plane defined by the intersection of van der Waals spheres, ρ is unity (bar packing), whereas in the other directions $\rho = 0.7405$ (close packing of atomic spheres). The area of the base of the spherical segment cut from the van der Waals sphere distance r from its center is $\pi(R^2 - r^2)$, and the surface area of the van der Waals sphere is $4\pi R^2$. The ratio of these values is $\sigma = (R^2 - r^2)/4R^2$; for N_c sections, we have $\bar{S} = \sigma N_c$. The total packing factor is then given by

$$\rho^* = \bar{S} \times 1.00 + (1 - \bar{S}) \times 0.7405. \quad (11)$$

This model can be checked as follows: With increasing N_c, $\bar{S}$ approaches unity, attaining it at $N_c = 12$: $\bar{S} = 12(R^2 - r^2)/4R^2$. Therefore,

$$R = (3/2)^{1/2} r. \quad (12)$$

Table 4 presents the results of calculations using Eq. (12) and the metallic radii (r) for $N_c = 12$ [3, 36], except for Cu, Zn, Cd, Hg (metallic radii corrected by the Pauling method for the divalent state), Group V and VII transition metals, Ga, In, Tl, Cr, Fe, Co, Ni, Rh, Ir (trivalent state), Mo, and W (tetravalent state).

It can be seen from Tables 2 and 4 that the values calculated by Eq. (12) agree with independent determinations to within 5–10%. This is the accuracy to which the packing factor in inorganic substances can be determined using Eq. (11).

The accuracy of relation (11) can also be assessed from the scatter in the ρ of isostructural crystals. In the diamond structure, the atomic volume is

$$V_a = \frac{\pi}{3}[4R^3 - 4(R - r)^2(2R + r)], \quad (13)$$

which is equal to the van der Waals atomic volume minus four segments cut distance r from the center. Since we use here $R = R_{IC} = 1.633r$, and $r = 0.772$, 1.176, 1.225, and 1.405 Å in the tetrahedral structures of C, Si, Ge, and Sn, respectively [37], V_a is 5.10, 18.02, 20.36, and 30.73 Å^3, respectively, or 0.90 of the unit-cell volume per atom in all cases. In the graphite structure, $V_a = 8.797$ Å^3, $R = 1.677$ Å, and $r = 0.760$ Å; V_0 can be calculated by an equation analogous to (13) in which three, rather than four, segments are subtracted from the van der Waals volume, because of the threefold coordination of carbon. In this way, we find $V_0 = 7.769$ Å^3 and $\rho^* = 0.88$. This small difference in ρ^* between diamond and graphite is better correlated with the low energy of the phase transition (0.3% of the atomization energy) than the large (by a factor of 2) difference in the classical (covalent) packing factors: 0.34 and 0.17.

Table 4. Van der Waals radii (Å) of metals calculated by Eq. (12)

M	R	M	R	M	R	M	R
Li	1.90	B	1.20	P	1.63	Br	1.73
Na	2.32	Al	1.75	As	1.81	I	1.98
K	2.88	Ga	1.75	Sb	2.03	Mn	1.66
Rb	3.04	In	1.96	Bi	2.17	Tc	1.73
Cs	3.27	Tl	1.98	V	1.72	Re	1.75
Cu	1.73	Sc	1.98	Nb	1.86	Fe	1.65
Ag	1.77	Y	2.20	Ta	1.87	Co	1.64
Au	1.86	La	2.29	S	1.73	Ni	1.63
Be	1.38	Si	1.68	Se	1.90	Ru	1.81
Mg	1.96	Ge	1.77	Te	2.14	Rh	1.75
Ca	2.41	Sn	1.99	Cr	1.67	Pd	1.86
Sr	2.63	Pb	2.09	Mo	1.76	Os	1.83
Ba	2.71	Ti	1.80	W	1.77	Ir	1.77
Zn	1.77	Zr	1.96	Th	2.20	Pt	1.87
Cd	1.98	Hf	1.94	U	2.14		
Hg	1.98						

Table 5. Van der Waals radii (Å) calculated from molar volumes of condensed substances

A	V_0, Å^3	r, Å	$\bar{S}$	ρ*	R	R_{cr}
F	16.05	0.745	0.191	0.790	1.536	1.42–1.62
Cl	27.53	0.997	0.174	0.786	1.810	1.66–1.92
Br	31.88	1.150	0.156	0.781	1.875	1.66–1.99
I	40.90	1.358	0.136	0.776	2.013	1.78–2.16
O	17.35	0.604	0.215	0.796	1.627	1.63–1.71
S(ortho)	25.78	1.020	0.359	0.834	1.924	1.63–1.85
S(monocl)	26.46	1.030	0.359	0.834	1.940	
Se(hex)	27.27	1.187	0.296	0.817	1.860	1.72
Se(monocl)	29.81	1.168	0.320	0.824	1.949	1.74–2.00
Te(hex)	33.97	1.417	0.230	0.800	1.930	1.75
γ-N	16.26	0.549	0.221	0.798	1.607	1.64–1.72
P	19.03	1.115	0.438	0.855	1.730	1.796
α-As	21.52	1.258	0.342	0.829	1.706	1.56
α-Sb	30.21	1.454	0.320	0.824	1.921	1.68
α-Bi	35.39	1.536	0.296	0.817	1.974	1.76

Using the known covalent bond lengths and molar volumes of Group V–VII nontransition elements in the crystalline state and solving coupled Eqs. (11) and (13), one can determine R and the corresponding σ and ρ*. Table 5 lists the values of V_0 and r taken from [18, 38], R and ρ* calculated as described above, and R extracted from XRD data. It can be seen that the mean packing factor is 0.788 (±1%) for isostructural A_2 molecules and 0.826 (±1.7%) for the ring and framework structures of the Group V and VI nontransition elements, whereas the ρ calculated for the A_2 molecules by the classical method from covalent radii ranges from 0.043 to 0.256,

Table 6. Molar volumes, bond lengths, and atomic and van der Waals radii in AX_4 crystals

AX_4	V_0, Å^3	d(A–X), Å	r_A, Å	r_X, Å	R_X, Å
CF_4(I)	66.4				1.507
CF_4(II)	65.7	1.3145	0.8022	0.5123	1.500
SiF_4	79.2	1.593	1.148	0.4255	1.512
GeF_4	82.5	1.689	1.390	0.4501	1.388
CCl_4(I)	145.0				1.925
CCl_4(II)	131.6	1.773	0.8173	0.9557	1.851
$SiCl_4$	143.9	2.008	1.196	0.8119	1.859
$SnCl_4$	162.1	2.275	1.436	0.8394	1.853
CBr_4(I)	171.5				2.022
CBr_4(II)	159.3	1.913	0.8063	1.107	1.964
$GeBr_4$	181.8	2.272	1.276	0.9961	1.998
$SnBr_4$	194.9	2.405	1.447	0.9930	1.986
CI_4	191.0	2.155	0.8029	1.352	2.060
SiI_4	160.3	2.43	1.229	1.201	2.114
GeI_4	161.1	2.498	1.276	1.222	2.097
SnI_4	171.1	2.667	1.448	1.219	2.100

with an average of 0.135 (±56%), and the ρ for the other structures ranges from 0.172 to 0.429, with an average of 0.303 (±32%). Thus, the scatter in ρ* is much smaller than that in ρ.

The molar volume method can also be used to determine the van der Waals radii of the halogens in AX_4 molecules by calculating the volumes of these molecules by the equation

$$V_m = \frac{4\pi}{3}\langle[R_A^3 - (R_A - r_A)^2(2R_A + r_A)] + [4R_X^3 - (R_X - r_X)^2(2R_X + r_X)]\rangle \quad (14)$$

and equating them to the experimentally determined volume V_0 multiplied by 0.7405. Taking the average of the van der Waals radii of the Group IV nontransition elements [39] as R_A and the reduced orbital radii [27] as r, we calculated the R_X values listed in Table 6. These values coincide with the crystallographic van der Waals radii of halogens (Table 3).

EQUILIBRIUM VAN DER WAALS RADII OF ISOLATED ATOMS

The minimum in the potential of van der Waals interaction between two isolated atoms corresponds to an equilibrium van der Waals radius R_e. Since different interatomic potentials were used in calculations of the van der Waals energy [40], there is a significant scatter in the reported distance corresponding to $E = 0$ (Table 7). In view of this, R_e is sometimes regarded as merely an adjustable parameter [4, 5, 40].

Allinger *et al.* [41], using experimental R data for inert gases (G) and the effective charges of atomic cores, calculated, by an interpolation method, R_e for all chemical elements, which proved close to the values of R determined in [42] from the structural data for GM, GX, Zn_2, Cd_2, and Hg_2 molecules, in which the bonds are weak and the atoms are in a nearly isolated state. The more detailed results obtained later in [43, 44] were also in close agreement with the equilibrium radii.

An important point is that the distances in heteronuclear van der Waals molecules turned out to be larger than the sum of the van der Waals radii because of the polarization effects:

$$D_{AB} = R_A + R_B + \Delta R_{AB}, \quad (15)$$

where

$$\Delta R_{AB} = a[(\alpha_A - \alpha_B)/\alpha_A]^{2/3}. \quad (16)$$

Here, $a = 0.045$, α is the electronic polarizability, and $\alpha_A < \alpha_B$. Since the interatomic distances in AB van der Waals molecules (D_{AB}) are larger than $\frac{1}{2}(D_{AA} + D_{BB})$, the dissociation energy of heteronuclear molecules is less than half the sum of the energies of the corresponding homonuclear bonds [45, 46]. Recall that the length of normal chemical bonds is smaller than the sum of covalent radii, and the energy is higher than the additive

Table 7. Equilibrium van der Waals radii of nonmetals

Author, year	R_e, Å								
	H	F	Cl	O	S	N	P	C	Si
Allinger, 1976	1.50	1.60	1.95	1.65	2.00	1.70	2.05	1.80	2.10
Mundt *et al*., 1983	1.17			1.36				1.80	2.10
Himan *et al*., 1987				1.4	1.85	1.5		1.5	
Gavezzotti, 1993	1.17		1.77	1.4	1.8	1.5		1.75	
Parkani *et al*., 1994	1.35							1.80	1.90
Venturelli, 1994	1.28				1.85			1.60	
Cornell *et al*., 1995	1.49	1.75		1.66	2.00	1.85	2.10	1.91	
Schmidt, 1996	1.61			1.63				1.94	2.11
Gavezzotti, 1999	1.49	1.42	1.70	1.60	1.70	1.64		1.72	

Table 8. Van der Waals radii (Å) of isolated atoms

A	R^0	R_G	R_e	A	R^0	R_G	R_e
H	1.96	1.56	1.56	C	1.85	2.05*	1.97
Li	2.72	2.7	2.46	Si	2.25	2.0	2.27
Na	2.82	2.8	2.68	Ge	2.23		2.42
K	3.08	2.9	3.07	Sn	2.34		2.57
Rb	3.22	3.0	3.23	Pb	2.34		2.72
Cs	3.38	3.1	3.42	Nb	2.50		2.41
Cu	2.30		2.24	Ta	2.44		2.41
Ag	2.34	2.0	2.41	N	1.70		1.88
Be	2.32		2.14	P	2.09		2.20
Mg	2.45	2.4	2.41	As	2.16		2.34
Ca	2.77		2.79	Sb	2.33		2.50
Sr	2.90		2.98	Bi	2.40		2.64
Ba	3.05		3.05	Cr	2.23		2.23
Zn	2.25	2.2	2.27	Mo	2.40		2.37
Cd	2.32	2.3	2.48	W	2.35		2.37
Hg	2.25	2.0	2.51	O	1.64		1.78
Sc	2.64		2.59	S	2.00	2.06	2.13
Y	2.73		2.69	Se	2.10		2.27
La	2.86		2.76	Te	2.30		2.42
B	2.05	1.7	2.06	Mn	2.29		2.22
Al	2.47		2.34	Re	2.38		2.35
Ga	2.38		2.44	Br	2.00	1.97	2.20
In	2.44	1.8	2.62	I	2.15	2.16	2.34
Tl	2.46	2.2	2.57	Fe	2.34		2.21
Ti	2.52		2.37	Co	2.30		2.21
Zr	2.63		2.52	Ni	2.26		2.20
Hf	2.54		2.51	Th	2.78		2.72
				U	2.80		2.50

* Calculated from data in [51].

Table 9. System of the van der Waals radii (Å) of elements

Li	Be											B	C	N	O	F
2.2	1.9											1.8	1.7	1.6	1.55	1.5
2.63	2.23											2.05	1.96	1.79	1.71	1.65
Na	Mg											Al	Si	P	S	Cl
2.4	2.2											2.1	2.1	1.95	1.8	1.8
2.77	2.42											2.40	2.26	2.14	2.06	2.05
K	Ca	Sc	Ti	V	Cr	Mn	Fe	Co	Ni	Cu	Zn	Ga	Ge	As	Se	Br
2.8	2.4	2.3	2.15	2.05	2.05	2.05	2.05	2.0	2.0	2.0	2.1	2.1	2.1	2.05	1.9	1.9
3.02	2.78	2.62	2.44	2.27	2.23	2.25	2.27	2.25	2.23	2.27	2.24	2.41	2.32	2.25	2.18	2.10
Rb	Sr	Y	Zr	Nb	Mo	Tc	Ru	Rh	Pd	Ag	Cd	In	Sn	Sb	Te	I
2.9	2.55	2.4	2.3	2.15	2.1	2.05	2.05	2.0	2.05	2.1	2.2	2.2	2.25	2.2	2.1	2.1
3.15	2.94	2.71	2.57	2.46	2.39	2.37	2.37	2.32	2.35	2.37	2.37	2.53	2.46	2.41	2.36	2.22
Cs	Ba	La	Hf	Ta	W	Re	Os	Ir	Pt	Au	Hg	Tl	Pb	Bi	Po	At
3.0	2.7	2.5	2.25	2.2	2.1	2.05	2.0	2.0	2.05	2.1	2.05	2.2	2.3	2.3		
3.30	3.05	2.81	2.52	2.42	2.36	2.35	2.33	2.34	2.37	2.41	2.25	2.53	2.53	3.52		
		Th	U													
		2.4	2.3													
		2.75	2.65													

value. Although this feature of van der Waals forces stems directly from the London–Kirkwood theory [26, 43, 46], it was not noticed until 1996; in 1998, this feature was confirmed by Alkorta *et al.* [47].

In spite of certain discrepancies, the van der Waals radii of all isolated atoms exceed the corresponding crystallographic radii by 10–30% [40, 48], which is commonly accounted for by the stronger interaction between molecules in solids [9]. At the same time, comparison of the separations in G_2 molecules and G crystals [42, 49] and $(X_2)_2$ condensed and gas-phase molecules, where the dissociation energies differ by an order of magnitude [46, 50], demonstrates that the van der Waals contact length is not determined by the interaction energy.

Since the van der Waals radii of hydrogen, carbon, and metals depend on bond polarity (difference in electronegativity) [see Eq. (10)], zero atomic charge corresponds to an isolated atom. Table 8 compares the Allinger's equilibrium radii (R_e), radii determined experimentally from the structure of molecules containing atoms of inert gases (R_G), and radii of elements in AX_n molecules reduced to zero charge on the metal atom (R^0). It can be seen that the van der Waals radii of isolated (neutral) atoms determined by different methods are in reasonable agreement, with allowance made for the possible experimental errors in R_G and R^0 and extrapolation errors in R_e. The largest discrepancy is observed in the case of hydrogen, because it has a flat potential curve, and its size varies markedly with even minor variations in the van der Waals interaction energy.

Table 9 presents the set of the recommended crystallographic (upper figures) and equilibrium (lower figures) van der Waals radii of elements.

ANISOTROPY IN VAN DER WAALS RADII

The above radii correspond to isotropic (spherical) atoms. At the same time, structural studies of crystalline iodine show that the intermolecular distance depends on the crystallographic direction [52]. Later studies [53] confirmed that the R of iodine is anisotropic; the effect was interpreted in terms of the electron-density distribution in the atoms forming the chemical bond. This result was also confirmed in other works [54–57]. However, Nyburg and Faerman [56] attributed the anisotropy in R to intermolecular interaction.

Whether the anisotropy in the van der Waals area of atoms is of intra- or intermolecular nature can be ascertained either by calculating the van der Waals configuration of isolated molecules or by experimentally determining the van der Waals shape of atoms in gas-phase molecules. The results of both approaches support Kitaigorodskii's conclusion.

Bader *et al.* [58] were the first to delineate the region containing 95% of the molecular charge. They found that, in isolated Li_2, B_2, C_2, N_2, O_2, and F_2 molecules, the van der Waals radius in the bond direction (longitudinal radius, R_l) is always smaller than the transverse

Table 10. Semiempirical estimates of the anisotropy in van der Waals radii (Å)

Atom	k_t	k_l	R_t	R_l'	R_l	R_t	R_l'	R_l
			equilibrium			crystallographic		
F	1.028	0.8294	1.75	1.60	1.41	1.54	1.42	1.24
Cl	1.037	0.7548	2.12	1.92	1.55	1.87	1.67	1.36
B	1.039	0.7287	2.23	2.00	1.57	1.97	1.77	1.38
I	1.040	0.7188	2.34	2.08	1.62	2.18	1.95	1.51
O	1.068	0.8253	1.92	1.58	1.48	1.65	1.37	1.28
S	1.089	0.7463	2.29	1.77	1.57	1.96	1.52	1.34
Se	1.095	0.7215	2.41	1.83	1.59	2.08	1.58	1.37
Te	1.097	0.7128	2.58	1.95	1.67	2.30	1.75	1.50
N	1.132	0.8188	2.15	1.48	1.55	1.87	1.28	1.35
P	1.170	0.7369	2.52	1.56	1.58	2.28	1.43	1.44
As	1.179	0.7112	2.65	1.62	1.60	2.42	1.47	1.46
Sb	1.182	0.7040	2.84	1.71	1.69	2.60	1.57	1.55

radius R_t. Later, the same was shown in calculations for AB, CO_2, C_2H_4, and C_2H_2 [59, 60].

The calculations by Ishikawa *et al.* [61] demonstrate that the anisotropy in the R of halogens depends on bond polarity in isolated molecules. For example, $R_t(F) = 1.456$ Å in KF and 1.344 Å in F_2 and $R_l(F) = 1.428$ Å in KF and 1.241 Å in F_2, with $\Delta R_{t-l} = 0.028$ Å in the ion pair and 0.103 Å in the covalent molecule. Similarly, $R_t(Cl) = 1.777$ Å in KCl and 1.696 Å in Cl_2 and $R_l(Cl) = 1.739$ Å in KCl and 1.510 Å in Cl_2, with $\Delta R_{t-l} = 0.038$ Å in the ion pair and 0.186 Å in the covalent molecule; $R_t(Br) = 1.894$ Å in KBr and 1.827 Å in Br_2 and $R_l(Br) = 1.853$ Å in KBr and 1.600 Å in Br_2, with $\Delta R_{t-l} = 0.041$ Å in the ion pair and 0.227 Å in the covalent molecule. Thus, with increasing covalence and bond polarizability, the anisotropy becomes more pronounced. The minimal anisotropy is observed in polar molecules. The anisotropy in the van der Waals radius was attributed to the formation of covalent bonds, which involves electron transfer from p_z orbitals to the bonding region, and, accordingly, a decrease in electron density at the opposite end of the orbitals. With decreasing bond covalence, the shift of electrons to the overlap region decreases; in ion pairs, there is no electron shift and, accordingly, no anisotropy.

Recent *ab initio* calculations for a large number of molecules [62] also showed that the anisotropy in the van der Waals radius depends on the effective charge on the atom. Unfortunately, no quantum-mechanical calculations have so far been performed for multielectron elements, which makes it difficult to draw general conclusions. This problem can be overcome, to some extent, by using semiempirical methods.

The outermost shell of isolated halogen atoms, characterized by R_e, contains seven electrons, which are uniformly distributed because there is no preferred direction. After the formation of an X_2 molecule with the participation of p_z electrons, the p_x and p_y orbitals, initially unoccupied, each contain two electrons and do not differ in this respect from the p orbitals of the corresponding anions, whereas, at the other end of the p_z orbital, there is electron deficiency (no electrons in the limit). These observations can be used to estimate R_t and R_l taking that the difference from R_e is caused by changes in the number of electrons in the outer shell from seven to eight and two, respectively. In terms of linear dimensions, these changes are described by the coefficients $(8/7)^{1/3} = 1.045$ and $(2/7)^{1/3} = 0.6586$ if the s and p electrons occupy equal volumes. Actually, these volumes are different, which can be easily taken into account using outer-shell orbital radii of elements [63]: From the volumes of the outer-shell s and p electrons, one evaluates the volume per electron (V_{e_s} and V_{e_p}). Next, one calculates the average volume per electron in two-, seven-, and eight-electron shells (^2V_e, ^7V_e, and ^8V_e) and the resultant coefficients for converting R_e into R_t and R_l:

$$k_t = 1.045(^8V_e/^7V_e)^{1/3} \text{ and } k_l = 0.6586(^2V_e/^7V_e)^{1/3}. \quad (17)$$

Table 10 lists the R_t and R_l calculated from the equilibrium and crystallographic radii using the coefficients given by (17).

With Eq. (17), we obtain the minimum R_l, since the electrons are assumed to have fully shifted from the periphery of the p_x orbital to the bonding region. The upper limit to R_l' can be evaluated under the assump-

Table 11. Experimentally determined anisotropic van der Waals radii (Å) in C–A bonds

A	R_t	R_l	ΔR	A	R_t	R_l	ΔR
H	1.26	1.01	025	S	2.03	1.60	0.43
F	1.38	1.30	0.08	Se	2.15	1.70	0.45
Cl	1.78	1.58	0.20	Te	2.33	1.84	0.49
Br	1.84	1.54	0.30	N	1.62	1.42	0.20
I	2.13	1.76	0.37	Sb	2.12	1.82	0.30
O	1.64	1.44	0.20	Bi	2.25	1.85	0.40

Table 12. Experimentally determined anisotropic van der Waals radii (Å) in A_2 molecules

A_2	R_t	R_l	ΔR	R_t	R_l	ΔR
	gas phase			solid phase		
H_2	1.70	1.52	0.18		1.52	
O_2	1.88	1.66	0.22	1.67	1.49	0.18
N_2	1.95	1.70	0.25	1.75	1.55	0.20
F_2		1.24		1.55	1.34	0.21
Cl_2	1.94	1.39	0.55	1.90	1.67	0.33
Br_2	2.05	1.37	0.68	2.01	1.64	0.37
I_2	2.20	1.36	0.84	2.16	1.76	0.40

tion that distortions of a van der Waals atom do not change its volume. In this way, we obtain

$$R_l' = R^3/R_t^2. \quad (18)$$

The data obtained using Eq. (18) (Table 10) are in qualitative agreement with more accurate calculations: the anisotropy increases with increasing atomic polarizability, and, accordingly, the difference in R_t is much larger than that in R_l. Moreover, the difference between the maximal and the minimal R_l decreases with increasing valence, indicating a reduction in the shift of the p_z-electron density to the bonding region.

The anisotropy in the van der Waals radii of hydrogen, oxygen, and halogens was first determined experimentally from the G–A interatomic distances in T-shaped GA_2 molecules [43, 44]. The R_t(A) radii thus found were, in all cases, larger than the isotropic R(A) inferred from the structure of GA molecules.

The anisotropy in van der Waals radii can also be assessed using optical data on the anisotropy in molecular polarizability. Since polarizability is proportional to the molecular volume, the cubic root of the ratio between the longitudinal (α_l) and transverse (α_t) axes of the bond (molecular) polarizability ellipsoid must be proportional to the linear dimension of the molecule. The longitudinal size of A_2 molecules is equal to the sum of the A–A distance and $2R_l$(A), and the transverse size is $2R_t$(A). Knowing the bond length and the R_t(A) (from the structures of GA_2 molecules), one can find R_l [64–66]. A similar approach was used to assess the anisotropy in the van der Waals area of atoms in more complex molecules (AX_2, BX_3, and AX_4) [67].

In condensed molecules, the anisotropy in R is governed by the intermolecular distances in different crystallographic directions. The corresponding results were obtained as early as 1953 by Kitaigorodskii [53]. More detailed data were reported in [56, 57] and, very recently, in [64–66] (Tables 11, 12).

Of crucial importance are the R_t of carbon atoms in single, double, and triple bonds (1.95, 2.01, and 2.17 Å, respectively [44]) and the R_l of hydrogen atoms in different chemical states (Table 11) [64].

The anisotropy in R sheds light on the mechanisms underlying the effect of bond orientation on the intermolecular distance [67–70] and the dependence of the hydrogen bond length on the bond angle [71]. The anisotropy complicates calculations of molecular structures; luckily, it is limited to atoms bonded to only one ligand. If an atom participates in two or more bonds making angles of 90° ± 30°, a radius which is longitudinal for one bond is transverse for another; as a result of this compensation, the atom remains spherical. This inference is supported by the example of CdX_2 molecules, in which the van der Waals radii are essentially isotropic.

INTERMEDIATE CASES BETWEEN COVALENT AND VAN DER WAALS RADII

Actual chemical bonding typically has an intermediate character, which reflects on interatomic distances. Experimental studies show that the bond lengths may vary from the sum of covalent radii to the sum of van der Waals radii, depending on the nature of the compound [72, 73]. In a number of works, the shortening of intermolecular distances was interpreted as evidence for a new type of interaction, which was called "specific," "secondary," or "interaction that cannot be described within the framework of the classical theory of chemical bonding." Actually, the variations in bond lengths are of crystal-chemical nature and can be understood in terms of the known concepts. They are due to the exchange (covalent) forces between molecules located in close proximity, which reduce the covalent bonding.

This was clearly shown in high-pressure studies of simple substances: the shortening of the distances between atomic chains in the structures of Se and Te was found to be accompanied by an increase in intrachain bond lengths [74–77]. Similar changes in bond lengths were observed in phosphorus, arsenic, antimony, and bismuth: high pressure caused contraction of the bonds between fragments of the covalent framework and elongation of the bonds within the fragments [78, 79]. Compression of halogen molecules was accompanied by a decrease in intermolecular distances and an increase in covalent bond lengths, to the extent that all interatomic distances became identical, as in the structure of metals [80].

Changes in interatomic distances in response to electron redistribution can be described within a classical crystal-chemical approach. As an example, consider a linear triatomic system, $I_1\cdots I_2\cdots I_3$. Figure 3 shows the plot of the intermolecular bond length D vs. intramolecular bond length d [72], and Table 13 lists the corresponding distances obtained by averaging experimental data. Since the D-vs.-d curve shows hyperbolic behavior [81], it can be described by the O'Keefe–Brese equation [82],

$$-\Delta d = 0.37 \ln n, \qquad (19)$$

where Δd is a change in d, and n is the bond order (ratio of the valence to the number of ligands, N_c). If the elongation of the intramolecular (short) bond I–I is caused by a partial transition of valence electrons to the intermolecular region, one can determine, using Eq. (19), which n corresponds to the particular intramolecular bond length, to find the intermolecular bond order N from $1 - n$, and then calculate, again using Eq. (19), the new bond length. The results of such calculations are presented in Table 13.

These data provide clear evidence for the transformation of the van der Waals bond into a covalent bond as a result of charge transfer. The change in the length of the covalent bond in the I_2 molecule upon the formation of the symmetrical system $I\cdots I\cdots I$ exactly corresponds to an increase in the coordination number of the central iodine atom from 1 to 2 ($n = 0.5$). Similar behavior is observed in the systems X–H···Y, Cl–Sb···Cl, X–Cd···X, Br–Br···Br, and S–S···S [72, 81, 83, 84].

Thus, the formation of a symmetrical three-center system from covalent and van der Waals bonds is equivalent to the transformation of a terminal bond into a bridge bond as a result of dimerization ($AX_n \longrightarrow A_2X_{2n}$), that is, to an increase in the covalent bond length by ≈0.13 Å and a decrease in the van der Waals distance by ≈0.67 Å (given that R is larger than r by about 0.80 Å). All the changes in interatomic distances observed to date fall within this range (increased by a factor of 2 to pass from radii to bond lengths).

As mentioned above, compression of molecular substances, e.g., condensed halogens, is also accompanied by an increase in covalent bond length and a decrease in intermolecular distance to the extent that they become identical. Equation (19) can be used to describe this process after modifying it to take into account the volume contraction of intermolecular contacts: the order of the bond resulting from a decrease in the van der Waals distance (N) must be increased by a factor of 3 to obtain the order of the "short" bond. The equalized distances can be found using a simple procedure: after subtracting the covalent bond length from the intermolecular distance, the obtained value Δd and Eq. (19) are used to determine N and $n = 1 - 3N$; then, Eq. (19) is used again to determine the increased length of the intramolecular bond. Knowing the covalent bond lengths in the condensed molecules Cl_2, Br_2, and I_2, one can choose bond orders to equalize the reduced intermolecular distance and the elongated intramolecu-

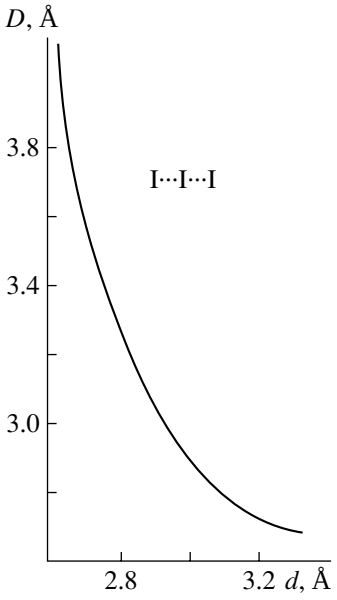

Fig. 3. Hyperbolic relationship between bond lengths in a three-center system.

Table 13. Lengths (Å) of covalent and van der Waals bonds I–I

d_{meas}	n	N	D_{calc}	D_{meas}
2.67	1.000	0.000	4.20	4.20
2.70	0.922	0.078	3.61	3.68
2.75	0.805	0.195	3.27	3.30
2.80	0.704	0.296	3.12	3.10
2.85	0.615	0.385	3.02	3.00
2.90	0.537	0.463	2.95	2.93
2.92	0.509	0.491	2.93	2.92

lar bond length. The equalized radii thus found are 1.245 Å for Cl, 1.40 Å for Br, and 1.62 Å for I. The experimentally determined values for Br and I are 1.41 and 1.62 Å, respectively [80]. For Cl, no molecule–metal transition has so far been observed. The strains and pressures at which such phase transitions occur were evaluated from the mechanical characteristics of these substances and coincided with experimental data to within 10% [22, 85, 86].

CONCLUSION

Systems of atomic radii were initially developed to calculate bond lengths, because their experimental determination required much effort and time. With the advent of modern XRD techniques, the need for *ab initio* calculations became less urgent, but precise knowledge of atomic radii became more important in interpreting the nature of the chemical bond. Comparison of an experimentally determined interatomic distance with the sum of the corresponding atomic radii makes it possible to assign a given chemical bond to one or another (or intermediate) type. The discovery, vital to structural chemistry, that the bond length may vary continuously from the van der Waals to the covalent value was also based on the comparison of measured distances with the sums of covalent and van der Waals radii. The extent of high-pressure phase transitions in molecular substances and the transition pressures are also governed by the van der Waals and covalent radii of the atoms involved.

The relationships, highlighted in this review, between the covalent, metallic, and van der Waals radii of elements are based on a large body of experimental data. Detailed data on the anisotropy in the atomic area in different states of aggregation are crucial for understanding the structure and nature of the chemical bond and necessary for quantum-chemical studies.

The use of experimental data on the structure of gas-phase molecules containing atoms of inert gases makes it possible to substantiate the concept of van der Waals radius and integrates crystal chemistry with other research areas.

REFERENCES

1. Mack, E., The Spacing of Non-Polar Molecules in Crystal Lattices: The Atomic Domain of Hydrogen, *J. Am. Chem. Soc.*, 1932, vol. 54, no. 6, pp. 2141–2165.
2. Magat, M., Über die "Wirkungsradien" gebundener Atome und den Orthoeffekt beim Dipolmoment, *Z. Phys. Chem.* (Munich), 1932, vol. 16, no. 1, pp. 1–18.
3. Pauling, L., *The Nature of the Chemical Bond*, Ithaca: Cornell Univ., 1960, 3rd ed.
4. Kitaigorodskii, A.I., *Organicheskaya kristallokhimiya* (Organic Crystal Chemistry), Moscow: Akad. Nauk SSSR, 1955.
5. Kitaigorodskii, A.I., *Molekulyarnye kristally* (Molecular Crystals), Moscow: Nauka, 1971.
6. Bondi, A., Van der Waals Volumes and Radii, *J. Phys. Chem.*, 1964, vol. 68, no. 3, pp. 441–451.
7. Bondi, A., The Heat of Sublimation of Molecular Crystals: Analysis and Molecular Structure Correlation, in *Condensation and Evaporation of Solids*, New York: Gordon and Breach, 1964.
8. Batsanov, S.S., Van der Waals Radii of Elements Evaluated from the Morse Equation, *Zh. Obshch. Khim.*, 1998, vol. 68, no. 4, pp. 529–534.
9. Zefirov, Yu.V. and Zorkii, P.M., Van der Waals Radii and Their Chemical Applications, *Usp. Khim.*, 1989, vol. 58, no. 5, pp. 713–746.
10. Zefirov, Yu.V. and Zorkii, P.M., New Chemical Applications of the van der Waals Radii, *Usp. Khim.*, 1995, vol. 64, no. 5, pp. 446–460.
11. Gavezzotti, A., The Calculation of Molecular Volume and the Use of Volume Analysis in the Investigation of Structured Media and of Solid-State Organic Reactivity, *J. Am. Chem. Soc.*, 1983, vol. 105, no. 16, pp. 5220–5225.
12. Filippini, G. and Gavezzotti, A., Empirical Intermolecular Potentials for Organic Crystals: The 6-exp Approximation Revisited, *Acta Crystallogr., Sect. B: Struct. Sci.*, 1993, vol. 49, no. 5, pp. 868–880.
13. Dunitz, J.D. and Gavezzotti, A., Attractions and Repulsions in Molecular Crystals, *Acc. Chem. Res.*, 1999, vol. 32, no. 8, pp. 677–684.
14. Wieberg, N., *Lehrbuch der anorganischen Chemie*, Berlin: Gruyter, 1995.
15. Rowland, R.S. and Taylor, R., Intermolecular Nonbonded Contact Distances in Organic Crystal Structures: Comparison with Distances Expected from van der Waals Radii, *J. Phys. Chem.*, 1996, vol. 100, no. 18, pp. 7384–7391.
16. Batsanov, S.S., Van der Waals Radii of Elements from Structural Inorganic Chemistry Data, *Izv. Akad. Nauk, Ser. Khim.*, 1995, no. 1, pp. 24–29.
17. Batsanov, S.S., Van der Waals Radii Evaluated from Structural Parameters of Metals, *Zh. Fiz. Khim.*, 2000, vol. 74, no. 7, pp. 1273–1276.
18. Pyykkö, P. and Straka, M., *Ab initio* Studies of the Dimers $(HgH_2)_2$ and $(HgMe_2)_2$: Metallophilic Attraction and van der Waals Radii of Mercury, *Phys. Chem. Chem. Phys.*, 2000, vol. 2, no. 11, pp. 2489–2493.
19. Cassidy, J.M. and Whitmire, K.H., Syntheses and Structures of the Phenylbismuth/Transition-Metal Carbonyl Compounds, *Inorg. Chem.*, 1991, vol. 30, no. 13, pp. 2788–2795.

20. Batsanov, S.S., Calculation of van der Waals Radii of Atoms from Bond Distances, *J. Mol. Struct.*, 1999, vol. 468, pp. 151–159.
21. Batsanov, S.S., Intramolecular Contact Radii Close to the van der Waals Radii, *Zh. Neorg. Khim.*, 2000, vol. 45, no. 6, pp. 992–996.
22. Batsanov, S.S., Thermodynamic Estimation of Dissociation Pressure Parameters for Solid Molecular Substances, *J. Phys. Chem. Solids*, 1992, vol. 53, no. 2, pp. 319–321.
23. Evans, C.J. and Gerry, M.C., The Pure Rotational Spectra of AuCl and AuBr, *J. Mol. Spectrosc.*, 2000, vol. 203, no. 1, pp. 105–117.
24. Anno, H., Koyanagi, T., and Matsubara, K., Epitaxial Growth of Zincblende MnTe Films as a New Magnetooptical Material, *J. Cryst. Growth*, 1992, vol. 117, pp. 816–819.
25. Batsanov, S.S., Atomic Radii of Elements, *Zh. Neorg. Khim.*, 1991, vol. 36, no. 12, pp. 3015–3037.
26. Tsirel'son, V.G., Chemical Bonding and Thermal Motion of Atoms in Crystals, *Itogi Nauki Tekh., Ser.: Kristallokhim.*, 1993, vol. 27.
27. Takeda, S., Inui, M., Tamaki, S., *et al.*, Electron Charge Distribution in Liquid Tellurium, *J. Phys. Soc. Jpn.*, 1993, vol. 62, no. 12, pp. 4277–4286.
28. Batsanov, S.S., Structural Features and Properties of Fluorine, Oxygen, and Nitrogen Atoms in Covalent Bonds, *Izv. Akad. Nauk SSSR, Ser. Khim.*, 1989, no. 2, pp. 67–70.
29. Batsanov, S.S., *Strukturnaya khimiya. Fakty i zavisimosti* (Structural Chemistry: Findings and Correlations), Moscow: Mosk. Gos. Univ., 2000.
30. Batsanov, S.S., Atomic Configurations in Tetrahalide Molecules, *Zh. Neorg. Khim.*, 2000, vol. 45, no. 12, pp. 2028–2031.
31. Montague, D.G., Chowdhury, M.R., Dore, J.C., and Reed, J.A., RISM Analysis of Structural Data for Tetrahedral Molecular Systems, *Mol. Phys.*, 1983, vol. 50, no. 1, pp. 1–23.
32. Jöllenbeck, K.M. and Weidner, J.U., X-ray Structural Study of the Liquid Silicon, Germanium, and Tin Tetrachlorides, *Ber. Bunsen–Ges. Phys. Chem.*, 1987, vol. 91, no. 1, pp. 17–24.
33. Misawa, M., Molecular Orientational Correlation in Liquid Halogens, *J. Chem. Phys.*, 1989, vol. 91, no. 6, pp. 2575–2580.
34. Ben-Amotz, D. and Herschbach, D.R., Estimation of Effective Diameters for Molecular Fluids, *J. Phys. Chem.*, 1990, vol. 94, no. 3, pp. 1038–1047.
35. Shil'nikov, V.I., Kuz'min, V.S., and Struchkov, Yu.T., Calculation of Atomic and Molecular Volumes and Areas, *Zh. Strukt. Khim.*, 1993, vol. 34, no. 4, pp. 98–106.
36. Batsanov, S.S., Metallic Radii of Nonmetals, *Izv. Akad. Nauk, Ser. Khim.*, 1994, no. 2, pp. 220–222.
37. Náray-Szabó, I., *Kristalykemia*, Budapest: Akadémiai Kiadó, 1969. Translated under the title *Neorganicheskaya kristallokhimiya*, Budapest: Hungarian Acad. Sci., 1969.
38. Donohue, J., *The Structure of the Elements*, New York: Wiley, 1974.
39. Chauvin, R., Explicit Periodic Trend of van der Waals Radii, *J. Phys. Chem.*, 1992, vol. 96, no. 23, pp. 9194–9197.
40. Allinger, N.L., Calculation of Molecular Structure and Energy by Force-Field Methods, *Adv. Phys. Org. Chem.*, 1976, vol. 13, pp. 1–82.
41. Allinger, N.L., Zhou, X., and Bergsma, J., Molecular Mechanics Parameters, *J. Mol. Struct.*, 1994, vol. 312, pp. 69–83.
42. Batsanov, S.S., Van der Waals Radii of Metals from Spectroscopic Data, *Izv. Akad. Nauk, Ser. Khim.*, 1994, no. 8, pp. 1374–1378.
43. Batsanov, S.S., On the Additivity of van der Waals Radii, *J. Chem. Soc., Dalton Trans.*, 1998, no. 5, pp. 1541–1545.
44. Batsanov, S.S., Structural Aspects of van der Waals Complexes, *Koord. Khim.*, 1998, vol. 24, no. 7, pp. 483–487.
45. Batsanov, S.S., Thermodynamic Aspects of the Formation of van der Waals Molecules, *Dokl. Akad. Nauk*, 1996, vol. 349, no. 3, pp. 340–342.
46. Batsanov, S.S., Some Aspects of van der Waals Interaction between Atoms, *Zh. Fiz. Khim.*, 1998, vol. 72, no. 6, pp. 1008–1011.
47. Alkorta, I., Rozas, I., and Elguero, J., Charge-Transfer Complexes between Dihalogen Compounds and Electron Donors, *J. Phys. Chem.*, 1998, vol. 102, pp. 9278–9285.
48. Allinger, N.L., Miller, M.A., Van Catledge, F.A., and Hirsch, J.A., The Calculation of the Conformation Structures of Hydrocarbons by the Westheimer–Hendrickson–Wiberg Method, *J. Am. Chem. Soc.*, 1967, vol. 89, no. 17, pp. 4345–4357.
49. Boese, R., Bläser, D., Heinemann, O., *et al.*, Evidence for Electron Density Features That Accompany the Noble Gases Solidification, *J. Phys. Chem.*, 1999, vol. 103, no. 31, pp. 6209–6213.
50. Runeberg, N. and Pyykkö, P., Relativistic Pseudopotential Calculations on Xe_2, RnXe, and Rn_2: The van der Waals Properties of Radon, *Int. J. Quantum Chem.*, 1998, vol. 66, no. 1, pp. 131–140.
51. Komissarov, A.V. and Heaven, M.C., Spectroscopy of the $A^2_\Delta - X^2_\Pi$ Transition of CH/D–Ar, *J. Chem. Phys.*, 2000, vol. 113, no. 5, pp. 1775–1780.
52. Harris, P.M., Mack, F., and Blake, F.C., The Atomic Arrangement in the Crystal of Orthorhombic Iodine, *J. Am. Chem. Soc.*, 1928, vol. 50, no. 6, pp. 1583–1600.
53. Kitaigorodskii, A.I., Khotsyanova, T.L., and Struchkov, Yu.T., On the Crystal Structure of Iodine, *Zh. Fiz. Khim.*, 1953, vol. 27, no. 6, pp. 780–781.
54. Zhdanov, G.S. and Zvonkova, Z.V., Evolution of Crystal-Chemical Views on the Nature of the Intermolecular Interaction and Intermolecular Radii Based on X-ray Diffraction Analysis, *Tr. Inst. Kristallogr.*, 1954, no. 10, pp. 71–78.
55. Bent, H.A., Structural Chemistry of Donor–Acceptor Interactions, *Chem. Rev.* (Washington, D. C.), 1968, vol. 68, no. 5, pp. 587–648.
56. Nyburg, S.C. and Faerman, C.H., A Revision of van der Waals Atomic Radii for Molecular Crystals: Nitrogen, Oxygen, Fluorine, Sulfur, Chlorine, Selenium, Bromine, and Iodine Bonded to Carbon, *Acta Crystallogr., Sect. B: Struct. Sci.*, 1985, vol. 41, no. 4, pp. 274–279.

57. Nyburg, S.C., Faerman, C.H., and Prasad, L., A Revision of van der Waals Atomic Radii for Molecular Crystals: II. Hydrogen Bonded to Carbon, *Acta Crystallogr., Sect. B: Struct. Sci.*, 1987, vol. 43, no. 1, pp. 106–110.

58. Bader, R.F.W., Henneker, W.H., and Cade, P.E., Molecular Charge Distributions and Chemical Binding, *J. Chem. Phys.*, 1967, vol. 46, no. 9, pp. 3341–3363.

59. Bader, R.F.W. and Bandrauk, A.D., Molecular Charge Distribution and Chemical Binding, *J. Chem. Phys.*, 1968, vol. 49, no. 4, pp. 1653–1675.

60. Bader, R.F.W., Carroll, M.T., Cheeseman, J.R., and Chang, C., Properties of Atoms in Molecules: Atomic Volumes, *J. Am. Chem. Soc.*, 1987, vol. 109, no. 26, pp. 7968–7979.

61. Ishikawa, M., Ikuta, S., Katada, M., and Sano, H., Anisotropy of van der Waals Radii of Atoms in Molecules: Alkali-Metal and Halogen Atoms, *Acta Crystallogr., Sect. B: Struct. Sci.*, 1990, vol. 46, no. 5, pp. 592–598.

62. Badenhoop, J.K. and Winhold, F., Natural Steric Analysis: *Ab initio* van der Waals Radii of Atoms and Ions, *J. Chem. Phys.*, 1997, vol. 107, no. 14, pp. 5422–5432.

63. Waber, J.T. and Cromer, D.T., Orbital Radii of Atoms and Ions, *J. Chem. Phys.*, 1965, vol. 42, no. 12, pp. 4116–4123.

64. Batsanov, S.S., Van der Waals Radii of Hydrogen in Gas-Phase and Condensed Molecules, *Struct. Chem.*, 1999, vol. 10, no. 6, pp. 395–400.

65. Batsanov, S.S., Anisotropy of van der Waals Atomic Radii in the Gas-Phase and Condensed Molecules, *Struct. Chem.*, 2000, vol. 11, no. 2/3, pp. 177–183.

66. Batsanov, S.S., Anisotropy in the van der Waals Area of Complex, Condensed, and Gas-Phase Molecules, *Koord. Khim.*, 2001, vol. 27, no. 11.

67. Dvorak, M.A., Ford, R.S., Suenram, R.D., *et al.*, Van der Waals vs Covalent Bonding: Microwave Characterization of a Structurally Intermediate Case, *J. Am. Chem. Soc.*, 1992, vol. 114, no. 1, pp. 108–115.

68. Klinkhammer, K.W. and Pyykkö, P., *Ab initio* Interpretation of the Closed-Shell Intermolecular Attraction in Dipnicogen and Dichalcogen Hydride Model Dimers, *Inorg. Chem.*, 1995, vol. 34, no. 16, pp. 4134–4138.

69. Leopold, K.R., Canagaratna, M., and Phillips, J.A., Partially Bonded Molecules from the Solid State to the Stratosphere, *Acc. Chem. Res.*, 1997, vol. 30, no. 2, pp. 57–64.

70. Aquilanti, V., Ascenzi, D., Bartolomei, M., *et al.*, The Nature of the Bonding in the O_2–O_2 Dimer, *J. Am. Chem. Soc.*, 1999, vol. 121, no. 46, p. 10794.

71. Lutz, H.D., Bonding and Structure of Water Molecules in Solid Hydrates: Correlation of Spectroscopic and Structural Data, *Struct. Bonding*, 1988, vol. 86, pp. 97–125.

72. Pyykkö, P., Strong Closed-Shell Interactions in Inorganic Chemistry, *Chem. Rev.* (Washington, D. C.), 1997, vol. 97, no. 5, pp. 597–636.

73. Batsanov, S.S., Effect of Intermolecular Distances on the Probability of Covalent Bonding, *Zh. Fiz. Khim.*, 2001, vol. 75, no. 4, pp. 754–756.

74. Keller, R., Holzapfel, W.B., and Schulz, H., Effect of Pressure on the Atom Position in Se and Te, *Phys. Rev. B: Solid State*, 1977, vol. 6, no. 10, pp. 4404–4412.

75. Isomäki, H.M. and von Boehm, J., Pressure Dependence of the Permittivity of Trigonal Se and Te, *Phys. Rev. B: Condens. Matter*, 1987, vol. 35, no. 15, pp. 8019–8023.

76. Parthasarathy, G. and Holzapfel, W.B., High-Pressure Structural Phase Transition in Tellurium, *Phys. Rev. B: Condens. Matter*, 1988, vol. 37, no. 14, pp. 8499–8501.

77. Akahama, Y., Kobayashi, M., and Kawamura, H., Pressure-Induced Structural Phase Transition in Sulfur at 83 GPa, *Phys. Rev. B: Condens. Matter*, 1994, vol. 48, no. 10, pp. 6862–6864.

78. Kikegawa, T. and Iwasaki, H., An X-ray Diffraction Study of Lattice Compression and Phase Transition of Crystalline Phosphorus, *Acta Crystallogr., Sect. B: Struct. Sci.*, 1983, vol. 39, no. 2, pp. 158–164.

79. Beister, H.J., Strössner, K., and Syassen, K., Rhombohedral to Simple-Cubic Phase Transition in Arsenic under Pressure, *Phys. Rev. B: Condens. Matter*, 1990, vol. 41, pp. 5535–5543.

80. Fujihisa, H., Fujii, Y., Takemura, K., and Shimomura, O., Structural Aspects of Dense Solid Halogens under High Pressure Studied by X-ray Diffraction—Molecular Dissociation and Metallization, *J. Phys. Chem. Solids*, 1995, vol. 56, no. 10, pp. 1439–1444.

81. Bürgi, H.B., Determination of the Stereochemistry of the Reaction Pathway from Crystal Structure Data, *Angew. Chem.*, 1975, vol. 87, no. 13, pp. 461–475.

82. O'Keefe, M. and Brese, N.E., Bond-Valence Parameters for Anion–Anion Bonds in Solids, *Acta Crystallogr., Sect. B: Struct. Sci.*, 1992, vol. 48, no. 2, pp. 152–154.

83. Zachariasen, W.H., The Crystal Structure of Monoclinic Metaboric Acid, *Actra Crystallogr.*, 1963, vol. 16, no. 5, pp. 385–389.

84. Dubler, E. and Linowski, L., Proof of the Existence of a Linear, Centrosymmetric Polyiodine Ion I_4^{2-}, *Helv. Chim. Acta*, 1975, vol. 58, no. 8, pp. 2604–2609.

85. Batsanov, S.S., Crystal-Chemical Evaluation of the Pressure of Polymorphic Transformations in Covalently Bonded Substances, *Zh. Strukt. Khim.*, 1993, vol. 34, no. 4, pp. 112–116.

86. Batsanov, S.S., Effect of High Pressure on Crystal Electronegativities of Elements, *J. Phys. Chem. Solids*, 1997, vol. 58, no. 3, pp. 527–532.